

HIJING can describe the anisotropy-scaled charge-dependent correlations at the Relativistic Heavy Ion Collider

Jie Zhao and Yicheng Feng

Department of Physics and Astronomy, Purdue University, West Lafayette, IN 47907, USA

Hanlin Li

*Hubei Province Key Laboratory of Systems Science in Metallurgical Process,
Wuhan University of Science and Technology, Wuhan, Hubei 430081, China*

Fuqiang Wang*

*Department of Physics and Astronomy, Purdue University, West Lafayette, IN 47907, USA and
School of Science, Huzhou University, Huzhou, Zhejiang 313000, China*

(Dated: June 1, 2021)

The experimentally measured charge-dependent correlations in heavy ion collisions have been suggested as a signature of the chiral magnetic effect (CME). Early model studies could not reproduce the measurement. For example, the Hijing model yielded far smaller magnitude for the charge-dependent correlation than observed in data. This led to the conclusion that the CME had to be invoked to explain the observed correlations in heavy ion collisions. In this paper we show that this conclusion of the CME interpretation is premature. We show that the reason that Hijing predicts a far smaller correlation than data is because the elliptic anisotropy (v_2) parameter in Hijing is too small. When properly scaled, the Hijing model can reproduce in entirety the measured correlations. We also employ the AMPT model, which has a large enough v_2 , to demonstrate that the measured data can be easily accommodated by models without invoking the CME.

I. INTRODUCTION

In recent years the chiral magnetic effect (CME) in relativistic heavy ion collisions has attracted intense interests [1–4]. The CME refers to an electric current along a strong magnetic field, produced in the early times of relativistic heavy ion collisions, perpendicular on average to the reaction plane (RP) of those collisions – the plane spanned by the impact parameter direction and the beam [5–10]. The electric current is a result of the motion of quarks in a metastable domain

*Electronic address: fqwang@purdue.edu

of imbalanced chirality, which can form from vacuum fluctuations in quantum chromodynamics (QCD) [11–13]. Such an electric current of quarks results in a charge separation in the final state across the reaction plane.

Reaction-plane and charge-dependent correlations have been observed in relativistic heavy ion collisions, first by the STAR experiment at BNL’s Relativistic Heavy Ion Collider (RHIC) [14–17] and later by experiments at the Large Hadron Collider (LHC) [18–21]. Some, but not all, of the observed features are consistent with charge separation from the CME. Background correlations due to mundane physics were studied and it was initially concluded that no model studied could reproduce the measurements [14, 15]. For example, the Hijing (Heavy ion jet interaction generator [22, 23]) model that was studied (where the real RP was used) yielded far smaller magnitude for the opposite-sign charge correlation than observed in data [14, 15]. This led to the conclusion that the CME had to be invoked to explain the observed correlations in heavy ion collisions [14, 15].

In this paper we show that this conclusion of the CME interpretation was premature. We show that the reason that Hijing predicts a far smaller correlation than data is because the elliptic anisotropy (v_2) [24] parameter in Hijing is too small. When properly scaled, the Hijing model can reproduce in entirety the measured correlations. We will also employ the AMPT (A multi-phase transport [25, 26]) model, which has a large enough v_2 , to demonstrate that the measured data can be easily accommodated by models without invoking the CME. Our studies reinforce the conclusion from other previous studies, contrary to that claimed in Refs [1, 14, 15], that background correlations may account for all of the observed correlations [16, 27–30].

II. THE HIJING AND AMPT MODELS

In this study, we use two typical, commonly used models, namely the Hijing (v1.411) and AMPT (v2.26t5d6) to calculate charge correlations. Hijing is a QCD inspired model simulating heavy ion collisions by binary nucleon-nucleon (NN) collisions using the Glauber geometry, incorporating nuclear shadowing effects and energy loss of partons traversing the medium created in those collisions (jet quenching). It uses PYTHIA [31, 32] for generating kinematic variables of scattered partons for each hard or semihard interaction and Lund string fragmentation (JETSET) [33] for hadronization. Jet quenching is included in our Hijing simulation.

We employ the string melting version of AMPT [25, 26] in our study. The model consists of four components: the initial condition of collisions, partonic elastic scatterings, hadronization and hadronic scatterings. The initial condition in AMPT is provided by the Hijing model. The

hadrons generated by Hijing are converted into valence quarks and antiquarks. The subsequent parton-parton elastic scatterings are described by ZPC [34]. The Debye-screened differential cross-section $d\sigma/dt \propto \alpha_s^2/(t - \mu_D^2)^2$ [26] is used for parton scattering. The strong coupling constant $\alpha_s = 0.33$ and Debye screening mass $\mu_D = 2.265/\text{fm}$ are employed, so that the total parton-parton scattering cross section is $\sigma = 3$ mb. After partons stop interacting, a simple quark coalescence model is applied to convert partons into hadrons [26, 35]. Subsequent interactions of those formed hadrons are modeled by ART [36]. Hadronic interactions include meson-meson, meson-baryon, and baryon-baryon elastic and inelastic scatterings. More details can be found in Ref. [26].

III. THE $\Delta\gamma$ CORRELATOR

The common observable to study the charge-dependent and reaction-plane-dependent azimuthal correlations is the $\Delta\gamma$ variable [37]. It is the difference of the opposite-sign (OS) and same-sign (SS) correlators,

$$\Delta\gamma = \gamma_{OS} - \gamma_{SS}, \quad (1)$$

such that one of the main physics backgrounds, the momentum conservation, is cancelled [14, 15]. The correlators are defined by

$$\gamma_{\alpha\beta} = \langle \cos(\phi_\alpha + \phi_\beta - 2\psi) \rangle, \quad (2)$$

where ϕ_α and ϕ_β are the azimuthal angles of two particles, either OS or SS, and ψ is the azimuthal angle of the reaction plane. The reaction plane is not measured, and is approximated by the event plane reconstructed from particle momenta in the final state. The inaccuracy is corrected by the event plane resolution. The event plane can also be taken as the direction of a single particle, called particle c . The resolution is simply given by the elliptic flow parameter of particle c , $v_{2,c}$. This is called the three-particle method [14, 15, 37]:

$$\gamma_{\alpha\beta} = \langle \cos(\phi_\alpha + \phi_\beta - 2\phi_c) \rangle / v_{2,c}, \quad (3)$$

Physics backgrounds arise when particles α and β are intrinsically correlated, not due to a global flow correlation to a common plane [27, 30, 37]. The intrinsic correlation is sometimes dubbed as nonflow correlation. One example is nonflow correlations due to resonance decays, primarily affecting OS correlations. In such a case, the background can be expressed as

$$\begin{aligned} \Delta\gamma_{\text{reso.}} &= \langle \cos(\phi_\alpha + \phi_\beta - 2\phi_{\text{reso.}}) \rangle \cdot v_{2,\text{reso.}} \\ &= \frac{N_{\text{reso.}}}{N_\alpha N_\beta} \langle \cos(\phi_\alpha + \phi_\beta - 2\phi_{\text{reso.}}) \rangle \cdot v_{2,\text{reso.}}, \end{aligned} \quad (4)$$

where $v_{2,\text{reso.}} = \langle \cos 2(\phi_{\text{reso.}} - \psi) \rangle$ is the resonance elliptic flow parameter. In the above equation, ϕ_α and ϕ_β are the azimuthal angles of the two decay daughters, so the quantity $\langle \cos(\phi_\alpha + \phi_\beta - 2\phi_{\text{reso.}}) \rangle$ is determined by decay kinematics, insensitive to collision centralities or types. Other nonflow background correlations include (mini)jets [38], or more generally, cluster correlations [27].

IV. RESULTS AND DISCUSSIONS

Figure 1 shows the γ_{OS} and γ_{SS} correlators in Hijing compared to experimental data [14, 15, 39]. The model data are binned in multiplicity similarly to experimental data to correspond to the cross-section fractions. The charged hadron multiplicity within pseudorapidity $-0.5 < \eta < 0.5$ is used. The multiplicity cut values are not the same between the models and the data, because the models do not exactly reproduce the data multiplicity and because of the detection inefficiencies in data that are not included in the models. The model and data results are plotted against the midrapidity charged hadron pseudorapidity density, $dN_{ch}/d\eta$. The decreasing γ amplitudes with increasing $dN_{ch}/d\eta$ is mainly due to the trivial multiplicity dilution effect. The γ_{OS} values from Hijing have the same sign as the experimental data. The γ_{SS} values are more different from the experimental data; γ_{SS} from Hijing are mostly positive, while the experimental data are mostly negative. The discrepancy between Hijing results and experimental data are mostly from the charge independent background, such as the momentum conservation effect [29, 40, 41].

To eliminate the charge-independent background sources, Fig. 2 shows the $\Delta\gamma$ correlator in Hijing. Further to remove the trivial multiplicity dilution effect and to better show the heavy ion data, the $\Delta\gamma$ is multiplied by $dN_{ch}/d\eta$ in Fig. 3. The Hijing results are compared to experimental data [14, 15, 39]. The Hijing results agree well with the data in small system $p+\text{Au}$ and $d+\text{Au}$ collisions. On the other hand, the Hijing results in $\text{Au}+\text{Au}$ collisions are much smaller than the data. This has been interpreted as a supporting evidence for the possible CME in experimental data [14, 15].

The $\Delta\gamma$ signal in Hijing is due to background correlations. According to Eq. (4), the background correlations are proportional to v_2 . In Fig. 4 we show the v_2 parameters from Hijing and compare them to those from experimental data [14, 15, 39]. Indeed, the v_2 values are similar between Hijing and data in small-system collisions, so the $\Delta\gamma$ values are also similar. In heavy ion collisions, however, the v_2 values in Hijing are much smaller than data. Similarly, as shown in Fig. 3, the $\Delta\gamma$ values in Hijing are much smaller than data too.

According to Eq. (4), the source of the background is the correlation term, $\langle \cos(\phi_\alpha + \phi_\beta -$

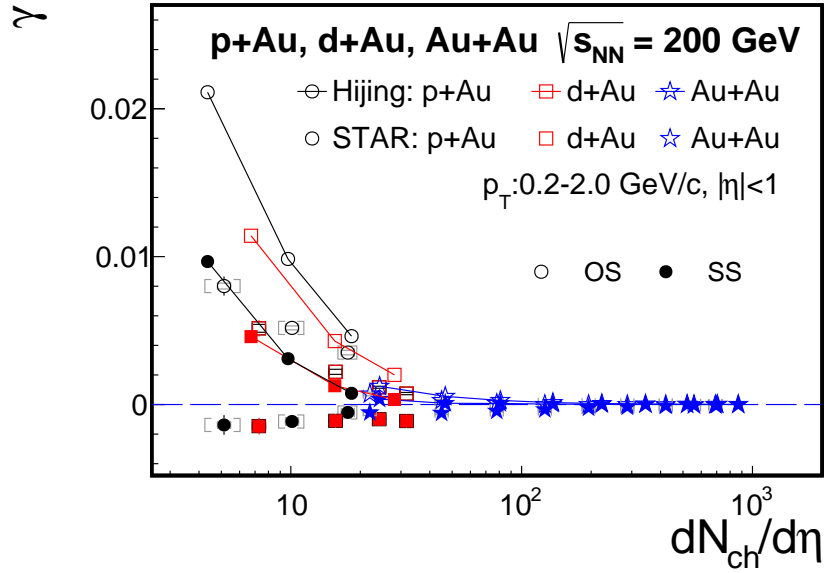


FIG. 1: Hijing predictions of the opposite-sign (OS, open symbols) and same-sign (SS, filled symbols) γ correlators, with comparisons to data [14, 15, 39]. The model predictions are connected by lines. The data symbols are same as the corresponding model symbols, but not connected by lines. The p +Au results are shown in circles, d +Au in squares, and Au+Au in stars. The results are plotted as functions of the mid-rapidity charged hadron multiplicity density, $dN_{ch}/d\eta$.

$2\phi_{\text{reso.}})$). This term reflects the intrinsic correlation between particles, such as the daughter particles from a resonance decay. In the background picture, therefore, the more direct quantity is the scaled correlator

$$\Delta\gamma_{\text{scaled}} = dN_{ch}/d\eta \cdot \Delta\gamma/v_2 \propto \frac{dN_{\text{reso.}}/d\eta}{dN_{ch}/d\eta} \langle \cos(\phi_\alpha + \phi_\beta - 2\phi_{\text{reso.}}) \rangle. \quad (5)$$

Figure 5 shows the scaled $\Delta\gamma_{\text{scaled}}$ correlator from Hijing, compared to data. Now there is not much difference between Hijing and data, unlike those shown in Fig. 2 and Fig. 5. Furthermore, there is not much difference overall in this quantity between small systems and big systems. This makes sense because the intrinsic particle correlations reflect the underlying physics mechanisms for the correlations, such as the decay kinematics, and should not be very different between different systems.

Also shown in Fig. 5 are the corresponding results from AMPT. In heavy-ion collisions the scaled $\Delta\gamma_{\text{scaled}}$ correlator in AMPT is also similar to data. The v_2 in AMPT, in contrast to Hijing, is known to reproduce data well [35].

Quantitatively, however, the models do not reproduce the data. The Hijing $\Delta\gamma_{\text{scaled}}$ overpredicts

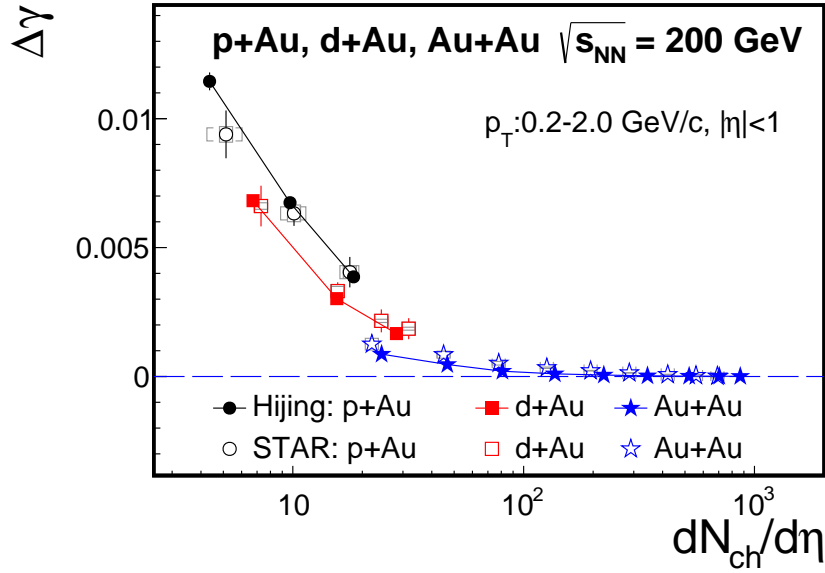


FIG. 2: Hijing predictions of the $\Delta\gamma$ correlator (filled symbols), with comparisons to data (open symbols) [14, 15, 39]. The model predictions are connected by lines. The p +Au results are shown in circles, d +Au in squares, and Au+Au in stars. The results are plotted as functions of the mid-rapidity charged hadron multiplicity density, $dN_{ch}/d\eta$.

Au+Au data, whereas the AMPT underpredicts the Au+Au data by a similar amount. The Hijing seems to well reproduce the small system data, but AMPT predicts a significantly weaker magnitude. These discrepancies could arise from a number of reasons. (1) Hadronic rescatterings can destroy resonances, and this could be a reason why the Au+Au data are lower than Hijing which does not include hadronic rescatterings. AMPT could have too many rescatterings resulting in weaker correlations. It is also possible that the reason is due to the lack of minijet correlations or that too few resonances are included in AMPT. On the other hand, hadronic rescattering would yield a decreasing correlation with increasing centrality, which is at odd with the Au+Au results in Fig. 5, but there could be other effects compensating a decreasing trend. (2) The fact that Hijing reproduces the small system data well may indicate that the minijet correlations are modeled well by Hijing. The Hijing results keep increasing with $dN_{ch}/d\eta$ in small systems, and this could be due to increasing jet correlations biased by the requirement of the high multiplicities [42]. The increase in the data is not as significant, perhaps due to the rescattering effect aforementioned. (3) The AMPT results in small systems are a factor of several lower than the data. This is likely due to the fact that minijet correlations are destroyed in the AMPT initialization using Hijing output. It

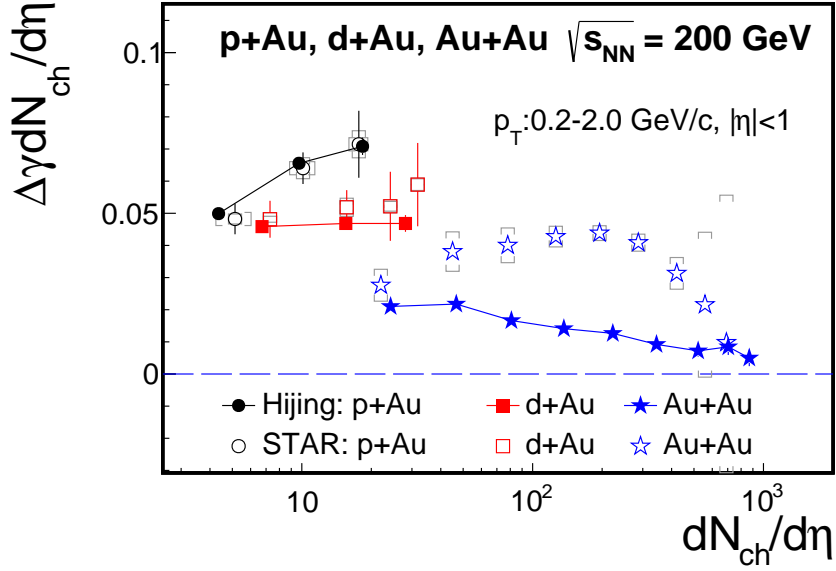


FIG. 3: Hijing predictions of the multiplicity scaled correlator (filled symbols), with comparisons to data (open symbols) [14, 15, 39]. The model predictions are connected by lines. The p +Au results are shown in circles, d +Au in squares, and Au+Au in stars. The results are plotted as functions of the mid-rapidity charged hadron multiplicity density, $dN_{ch}/d\eta$.

is unclear why the overall correlation strengths differ by a factor of 2 or so between small systems and heavy ion collisions in AMPT, unlike Hijing. Further investigation is needed.

Note that the backgrounds arise from correlations of the background sources with the reconstructed event plane or the third particle c , and thus are propagated into the three-particle correlator. The physics nature of the correlations with the event plane or the particle c is unimportant for the background explanation of the $\Delta\gamma$ correlator. For example, the correlation to the event plane or c in Hijing is likely due to jets (e.g. a resonance and the particle c are parts of a dijet) or multiparticle clusters (e.g. from string decays); the correlation to event plane or c in AMPT is likely due to collective elliptic flow, at least for heavy ion collisions, such that almost all particles of the event are correlated.

V. SUMMARY

The background contamination in the CME-sensitive $\Delta\gamma$ observable arises from intrinsic particle correlations (nonflow). Those nonflow correlations include resonance decays, clusters of multiparticle correlations, and (mini)jets. We employed the Hijing and AMPT models to study the effect

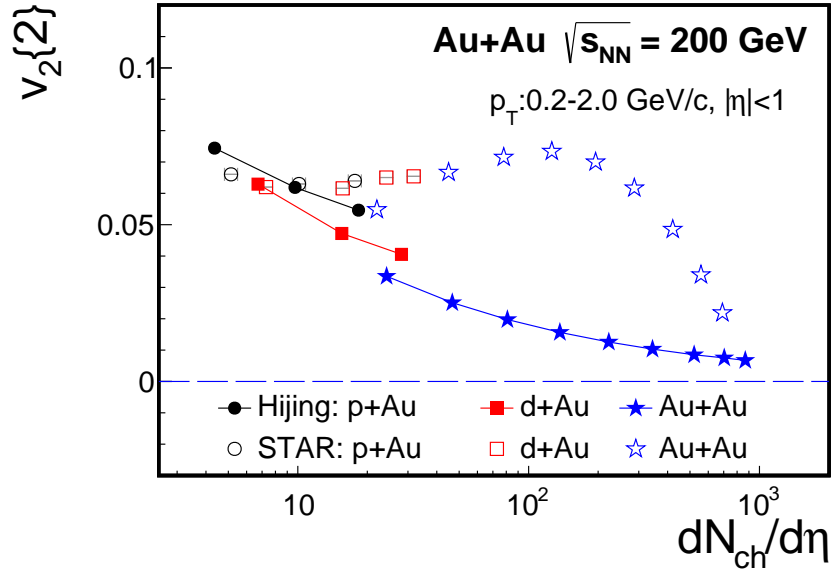


FIG. 4: Hijing predictions of the v_2 parameter (filled symbols), with comparisons to data (open symbols) [39]. The model predictions are connected by lines. The p +Au results are shown in circles, d +Au in squares, and Au+Au in stars. The results are plotted as functions of the mid-rapidity charged hadron multiplicity density, $dN_{ch}/d\eta$.

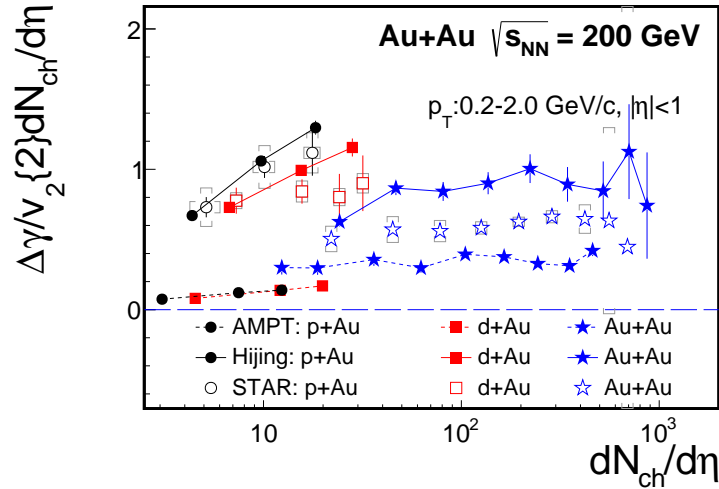


FIG. 5: Hijing and AMPT predictions of the scaled correlator, $dN_{ch}/d\eta \cdot \Delta\gamma/v_2$ (filled symbols), with comparisons to data (open symbols) [39]. The Hijing predictions are connected by solid lines and the AMPT results are connected by dashed lines. The p +Au results are shown in circles, d +Au in squares, and Au+Au in stars. The results are plotted as functions of the mid-rapidity charged hadron multiplicity density, $dN_{ch}/d\eta$.

of those backgrounds. Hijing seems to contain similar strength of those backgrounds as in data. Because of the weaker correlation to event plane or c , the final $\Delta\gamma$ observable in Hijing is much smaller than the heavy ion data. If the collective flow was present in Hijing, then the data would be well reproduced as indicated by the comparisons of the scaled $\Delta\gamma_{\text{scaled}}$ correlator. AMPT, on the other hand, does not seem to contain enough correlations as in data as indicated by the small system results. This could be due to the fact that minijets are not included in AMPT, not all high mass resonances are included, and/or resonance decay daughters rescatter and lose their correlations from decay. As a result, although AMPT has enough v_2 , the $\Delta\gamma$ values in AMPT are underpredicted.

The models do not necessarily reproduce data exactly. However, one cannot conclude that there must be CME in the heavy ion data just because the data $\Delta\gamma$ is larger than that in models. In the case of AMPT, this would not explain the small system results where any CME would be small, yet AMPT is off from data by a large amount. The reason Hijing does not reproduce data in terms of $\Delta\gamma$ is because Hijing does not have enough v_2 . There have been claims that the CME had to be invoked because no model studied, including Hijing, could reproduce data. This conclusion was premature as we have demonstrated in this work.

The physics backgrounds are dominant in the CME-sensitive $\Delta\gamma$ observable. When backgrounds dominate, one should be careful not to overly rely on models. Models in this case are useful only to guide one's thinking, but cannot be used for quantitative predictions of the backgrounds. This is because a small deviation of the model from reality could give a large error on the extracted signal from data treating the model as background, potentially leading to a wrong conclusion. Backgrounds have to be rigorously subtracted by data-driven methods before any conclusion about the CME can be made [20, 21, 43, 44].

Acknowledgments

We thank Dr. Wei Li for fruitful discussions. This work is supported in part by US Department of Energy Grant No. DE-SC0012910, the National Natural Science Foundation of China under Grant No. 11847315, 11947410 and the Natural Science Foundation of Hubei Province under Grant No. 2019CFB563.

[1] D. E. Kharzeev, J. Liao, S. A. Voloshin, and G. Wang. *Prog. Part. Nucl. Phys.*, 88:1–28, 2016.

- [2] Jie Zhao. *Int. J. Mod. Phys. A*, 33(13):1830010, 2018.
- [3] Jie Zhao, Zhoudunming Tu, and Fuqiang Wang. Status of the chiral magnetic effect search in relativistic heavy-ion collisions. *Nucl. Phys. Rev.* 35. 03. 225, 2018.
- [4] Jie Zhao and Fuqiang Wang. Experimental searches for the chiral magnetic effect in heavy-ion collisions. *Prog. Part. Nucl. Phys.*, 107:200–236, 2019.
- [5] Dmitri Kharzeev. Parity violation in hot QCD: Why it can happen, and how to look for it. *Phys. Lett. B*, 633:260–264, 2006.
- [6] Dmitri E. Kharzeev, Larry D. McLerran, and Harmen J. Warringa. The Effects of topological charge change in heavy ion collisions: 'Event by event P and CP violation'. *Nucl. Phys. A*, 803:227–253, 2008.
- [7] Kenji Fukushima, Dmitri E. Kharzeev, and Harmen J. Warringa. *Phys. Rev. D*, 78:074033, 2008.
- [8] Berndt Muller and Andreas Schafer. Charge Fluctuations from the Chiral Magnetic Effect in Nuclear Collisions. *Phys. Rev. C*, 82:057902, 2010.
- [9] K. F. Liu. Charge-dependent Azimuthal Correlations in Relativistic Heavy-ion Collisions and Electromagnetic Effects. *Phys. Rev. C*, 85:014909, 2012.
- [10] Dmitri E. Kharzeev. The Chiral Magnetic Effect and Anomaly-Induced Transport. *Prog. Part. Nucl. Phys.*, 75:133–151, 2014.
- [11] T. D. Lee and G. C. Wick. Vacuum Stability and Vacuum Excitation in a Spin 0 Field Theory. *Phys. Rev. D*, 9:2291–2316, 1974.
- [12] Dmitri Kharzeev, R. D. Pisarski, and Michel H. G. Tytgat. *Phys. Rev. Lett.*, 81:512–515, 1998.
- [13] Dmitri Kharzeev and Robert D. Pisarski. Pionic measures of parity and CP violation in high-energy nuclear collisions. *Phys. Rev. D*, 61:111901, 2000.
- [14] B. I. Abelev et al. Azimuthal Charged-Particle Correlations and Possible Local Strong Parity Violation. *Phys. Rev. Lett.*, 103:251601, 2009.
- [15] B. I. Abelev et al. Observation of charge-dependent azimuthal correlations and possible local strong parity violation in heavy ion collisions. *Phys. Rev. C*, 81:054908, 2010.
- [16] L. Adamczyk et al. Fluctuations of charge separation perpendicular to the event plane and local parity violation in $\sqrt{s_{NN}} = 200$ GeV Au+Au collisions at the BNL Relativistic Heavy Ion Collider. *Phys. Rev. C*, 88(6):064911, 2013.
- [17] L. Adamczyk et al. Beam-energy dependence of charge separation along the magnetic field in Au+Au collisions at RHIC. *Phys. Rev. Lett.*, 113:052302, 2014.
- [18] Betty Abelev et al. Charge separation relative to the reaction plane in Pb-Pb collisions at $\sqrt{s_{NN}} = 2.76$ TeV. *Phys. Rev. Lett.*, 110(1):012301, 2013.
- [19] Vardan Khachatryan et al. Observation of charge-dependent azimuthal correlations in p -Pb collisions and its implication for the search for the chiral magnetic effect. *Phys. Rev. Lett.*, 118(12):122301, 2017.
- [20] Albert M Sirunyan et al. Constraints on the chiral magnetic effect using charge-dependent azimuthal correlations in p Pb and PbPb collisions at the CERN Large Hadron Collider. *Phys. Rev. C*, 97(4):044912, 2018.

- [21] Shreyasi Acharya et al. Constraining the magnitude of the Chiral Magnetic Effect with Event Shape Engineering in Pb-Pb collisions at $\sqrt{s_{NN}} = 2.76$ TeV. *Phys. Lett. B*, 777:151–162, 2018.
- [22] Xin-Nian Wang and Miklos Gyulassy. HIJING: A Monte Carlo model for multiple jet production in p p, p A and A A collisions. *Phys. Rev. D*, 44:3501–3516, 1991.
- [23] Xin-Nian Wang. pQCD based approach to parton production and equilibration in high-energy nuclear collisions. *Phys. Rept.*, 280:287–371, 1997.
- [24] W. Reisdorf and H. G. Ritter. Collective flow in heavy-ion collisions. *Ann.Rev.Nucl.Part.Sci.*, 47:663–709, 1997.
- [25] Bin Zhang, C. M. Ko, Bao-An Li, and Zi-wei Lin. A multiphase transport model for nuclear collisions at RHIC. *Phys. Rev., C* 61:067901, 2000.
- [26] Zi-Wei Lin, Che Ming Ko, Bao-An Li, Bin Zhang, and Subrata Pal. A Multi-phase transport model for relativistic heavy ion collisions. *Phys. Rev., C* 72:064901, 2005.
- [27] Fuqiang Wang. *Phys. Rev. C*, 81:064902, 2010.
- [28] Adam Bzdak, Volker Koch, and Jinfeng Liao. *Phys. Rev. C*, 81:031901, 2010.
- [29] Soren Schlichting and Scott Pratt. *Phys. Rev. C*, 83:014913, 2011.
- [30] Fuqiang Wang and Jie Zhao. Challenges in flow background removal in search for the chiral magnetic effect. *Phys. Rev. C*, 95(5):051901, 2017.
- [31] Torbjorn Sjostrand. The Lund Monte Carlo for Jet Fragmentation and e+ e- Physics: Jetset Version 6.2. *Comput. Phys. Commun.*, 39:347–407, 1986.
- [32] Torbjorn Sjostrand, Stephen Mrenna, and Peter Z. Skands. PYTHIA 6.4 Physics and Manual. *JHEP*, 05:026, 2006.
- [33] Bo Andersson, G. Gustafson, G. Ingelman, and T. Sjostrand. Parton Fragmentation and String Dynamics. *Phys. Rept.*, 97:31–145, 1983.
- [34] Bin Zhang. ZPC 1.0.1: A Parton cascade for ultrarelativistic heavy ion collisions. *Comput.Phys.Commun.*, 109:193–206, 1998.
- [35] Zi-Wei Lin. Evolution of transverse flow and effective temperatures in the parton phase from a multiphase transport model. *Phys.Rev.*, C90:014904, 2014.
- [36] Bao-An Li and Che Ming Ko. Formation of superdense hadronic matter in high-energy heavy ion collisions. *Phys.Rev.*, C52:2037–2063, 1995.
- [37] Sergei A. Voloshin. *Phys. Rev. C*, 70:057901, 2004.
- [38] Hannah Petersen, Thorsten Renk, and Steffen A. Bass. Medium-modified Jets and Initial State Fluctuations as Sources of Charge Correlations Measured at RHIC. *Phys. Rev., C* 83:014916, 2011.
- [39] J. Adam et al. Charge-dependent pair correlations relative to a third particle in p+Au and d+Au collisions at RHIC. *Phys. Lett.*, B798:134975, 2019.
- [40] Adam Bzdak, Volker Koch, and Jinfeng Liao. Azimuthal correlations from transverse momentum conservation and possible local parity violation. *Phys. Rev., C* 83:014905, 2011.
- [41] Scott Pratt, Soeren Schlichting, and Sean Gavin. Effects of Momentum Conservation and Flow on

- Angular Correlations at RHIC. *Phys. Rev. C*, 84:024909, 2011.
- [42] L. Adamczyk et al. Effect of event selection on jetlike correlation measurement in d +Au collisions at $\sqrt{s_{NN}} = 200$ GeV. *Phys. Lett.*, B743:333–339, 2015.
- [43] Haojie Xu, Jie Zhao, Xiaobao Wang, Hanlin Li, Ziwei Lin, Caiwan Shen, and Fuqiang Wang. *Chin. Phys. C*, 42:084103, 2018.
- [44] Jie Zhao, Hanlin Li, and Fuqiang Wang. Isolating the chiral magnetic effect from backgrounds by pair invariant mass. *Eur. Phys. J. C*, 79(2):168, 2019.